

# Ultra-broadband electromagnetic MEMS vibration energy harvesting

Huicong Liu<sup>1,2</sup>, Lokesh Dhakar<sup>2,3</sup> and Chengkuo Lee<sup>2</sup>

<sup>1</sup>Robotics and Microsystems Center, School of Mechanical & Electric Engineering, Soochow University, Suzhou, P. R. China

<sup>2</sup>Department of Electrical and Computer Engineering, National University of Singapore, Singapore

<sup>3</sup>NUS Graduate School for Integrative Sciences and Engineering, Singapore

E-mail: elelc@nus.edu.sg; hcliu078@suda.edu.cn

**Abstract.** This paper presents the design, fabrication and characterization of an electromagnetic MEMS energy harvester with ultra-broad operating bandwidth. The beam stretching induced nonlinear spring stiffness enables the resonance to extend from 65 Hz to 340 Hz and 400 Hz at accelerations of 0.5g and 1.0g, respectively. The ultra-wide bandwidth could benefit the harvester device for more efficient vibration energy harvesting.

## 1. Introduction

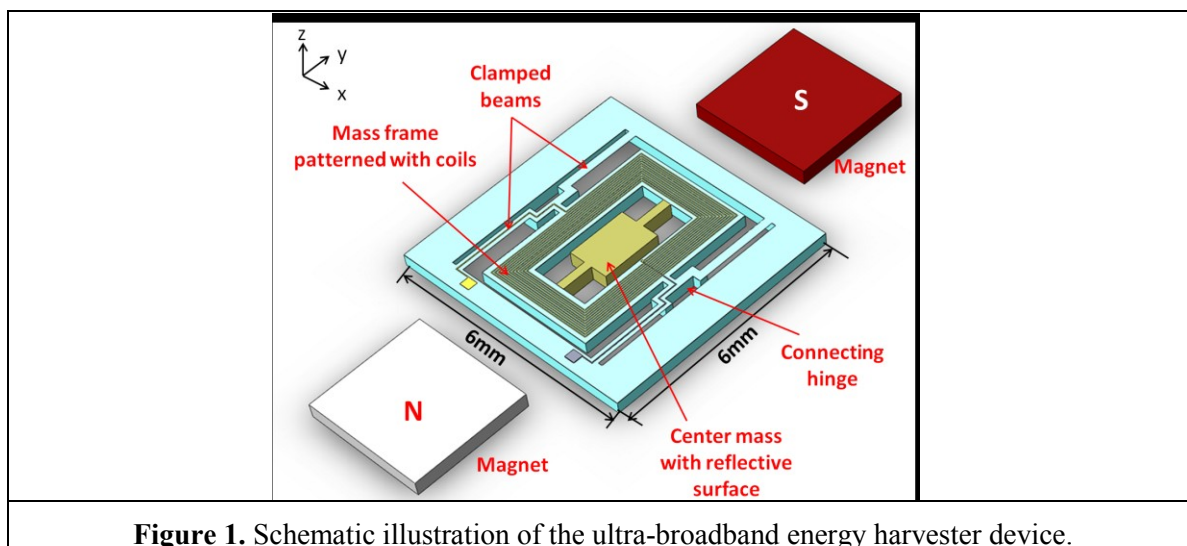
In the ambient environment, there are various vibration sources exhibiting in buildings, machines, transportations and human motions [1]. Generally, these vibration sources have random or irregular frequency peaks distributed in a certain bandwidth range. Vibration energy harvesting via electromagnetic, piezoelectric and electrostatic approaches have attracted more research attention for low-power electronics [2]. No matter which transduction mechanism was accomplished, most of the previous research work focused on the development of a linear oscillation system, where the maximum power output occurs at its resonant frequency. In the case that the ambient excitation frequency varies slightly, the output performance of the energy harvester can drop significantly. Since most of the vibration sources are present in a random or frequency varying scenario, it becomes a great challenge to broaden the operating bandwidth for more efficient vibration energy harvesting [3-4]. The use of nonlinear stiffness as a means to enlarge the bandwidth of energy harvesters has been reported by a number of works. They can be categorized into three main approaches, which are based on magnetic force [5-6], end-stopping of proof mass [7] and nonlinear beam stretching [8-9]. The first two approaches require extra assembly of bulk magnet or mechanical stoppers, thus they are usually implemented in macro-scale prototypes. Liu et al [10-11] have developed micro-scale broadband piezoelectric energy harvesters by incorporating the metal package base as the amplitude stopper of the MEMS PZT cantilever. Miki et al [12] have reported a MEMS in-plane electret energy harvester with nonlinear spring. The spring hardening effect can be induced as the silicon mass engages with the fixed-free secondary springs. For the nonlinear beam stretching method, Nguyen et al [13] have studied the spring hardening and softening behaviours of the broadband MEMS energy harvesting devices based on the design of special beam geometry. This work presents an ultra-broadband electromagnetic MEMS vibration energy harvester. The nonlinear beam stretching at three resonance



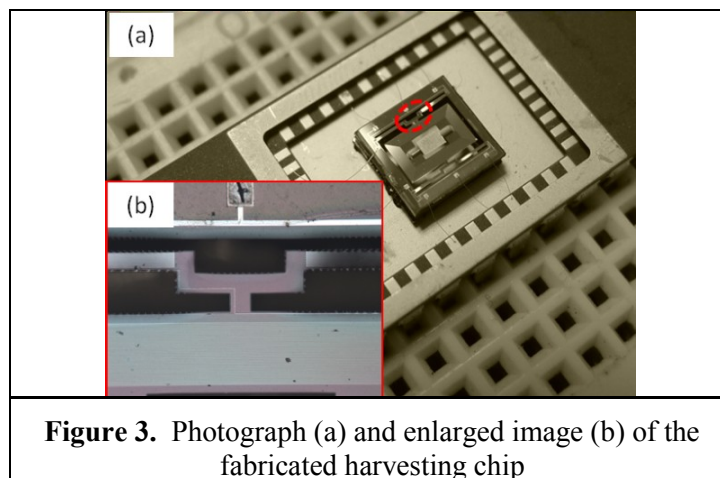
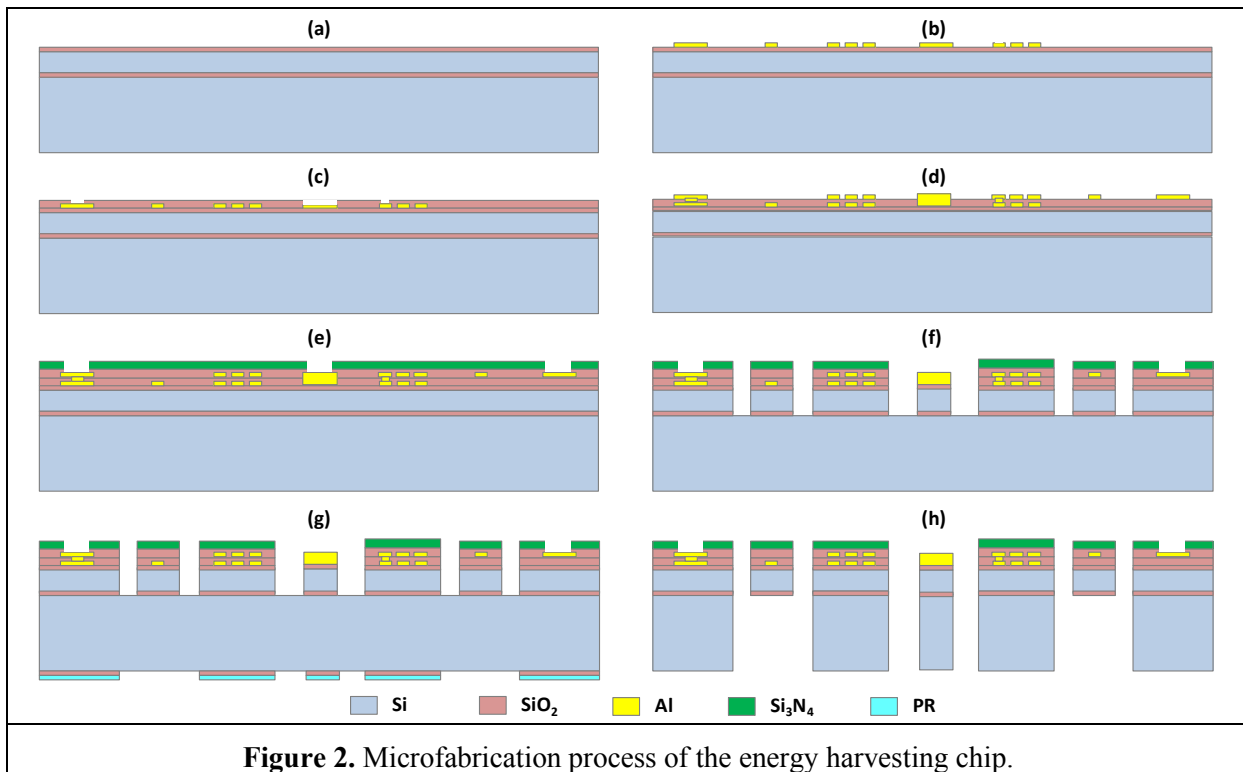
modes results in an ultra-wide range of operating frequencies compared to other nonlinear energy harvesting devices.

## 2. Device configuration and microfabrication

The schematic illustration of the ultra-broadband harvester device is shown in Fig. 1(a). It consists of two pairs of clamped beams which are connected to a mass frame through the connecting hinges at two sides. The length, width and thickness of each clamped beam are 1.9 mm, 0.2 mm and 3  $\mu\text{m}$ , respectively. The mass frame of 0.75 mm wide is patterned with metal coils of 5  $\mu\text{m}$  in width and 5  $\mu\text{m}$  in space. A pair of permanent magnets with two opposite poles is assembled such that a magnetic field along the  $y$ -direction is applied across the device. Hence, the electric current will be generated in the metal coils via the torsional vibrations of the mass frame along the connecting hinges. The center mass with reflective surface is used to observe the oscillating behaviour of the mass frame by the reflection of laser light. The wide bandwidth of the oscillation system can be explained by the Duffing stiffening induced by the clamped beam stretching during torsional and out-of-plane vibrations at resonances.



The energy harvesting chip of 6 mm $\times$ 6 mm $\times$ 0.4 mm is micro-fabricated by the micro-machining processes as shown in Fig. 2. It is first started by an 8 inch SOI wafer with 3  $\mu\text{m}$  device layer, 1.1  $\mu\text{m}$  buried oxide (BOX) layer and 725  $\mu\text{m}$  handle layer. In Fig. 2(a), a 0.2  $\mu\text{m}$  thermal oxide ( $\text{SiO}_2$ ) layer is initially deposited on the frontside surface by plasma-enhanced chemical vapour deposition (PECVD). Then physical vapour deposition, patterning and reactive ion etching (RIE) are conducted to form the first layer Al coils as shown in Fig. 2(b). In Fig. 2(c), 0.5  $\mu\text{m}$   $\text{SiO}_2$  layer is deposited by PECVD and pad opening is formed by RIE of  $\text{SiO}_2$ . It is followed by the deposition and patterning of a second layer of Al coils as shown in Fig. 2(d). In Fig. 2(e), the passivating layers of  $\text{SiO}_2$  and  $\text{Si}_3\text{N}_4$  of each 0.5  $\mu\text{m}$  thick are successively deposited by PECVD. This is followed closely by RIE to form pad opening and reflective surface. In Fig. 2(f), a series of RIE processes of  $\text{Si}_3\text{N}_4$ ,  $\text{SiO}_2$  and Si are conducted to define the frontside structural features. Later on, the SOI wafer is backside grinded and polished to be approximately 400  $\mu\text{m}$ . A 2  $\mu\text{m}$  PECVD  $\text{SiO}_2$  layer is deposited and patterned at the backside surface (in Fig. 2(g)) and backside Si deep reactive ion etch (DRIE) is followed to pattern and release the back structural features (in Fig. 2(h)). The DRIE process is conducted in a time-controlled manner so as to make sure the process is stopped effectively at the BOX layer. Figure 3 (a) is a photograph of the fabricated and packaged energy harvesting chip and (b) is an enlarged image of the clamped beams connected by hinge.

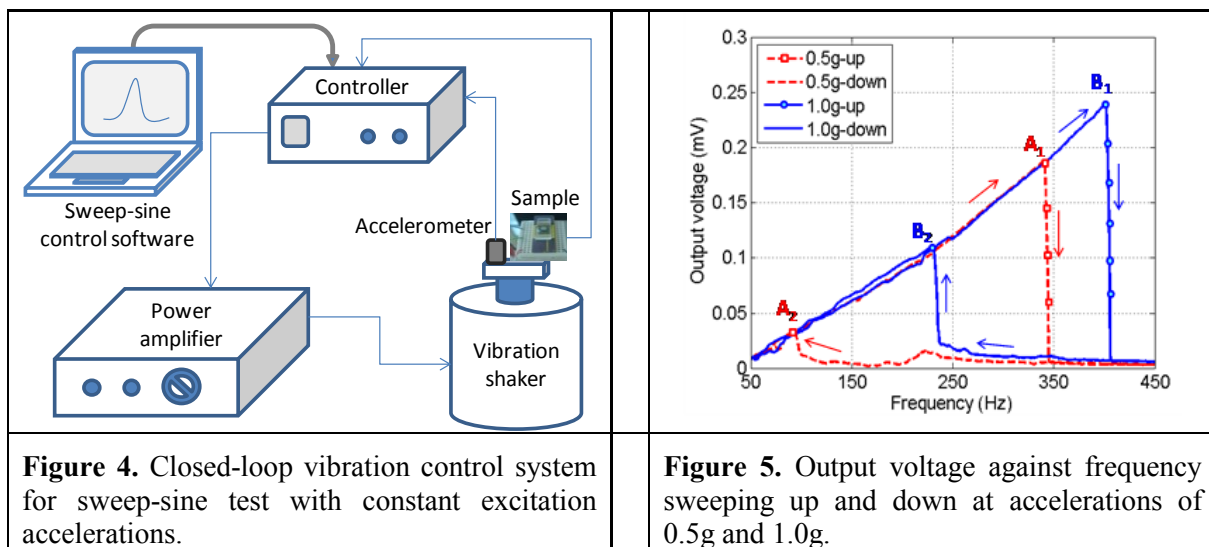


### 3. Experiment and results

The packaged device is tested by a closed-loop vibration control system as illustrated in Fig. 4, which is able to provide constant excitation accelerations to the harvester device. It consists of a vibration shaker driven by a controller through a power amplifier. An accelerometer is attached on the shaker to give the signal feedback to the controller. The controller is connected to a laptop installed with sweep-sine control software to perform a sweep-sine within a specific frequency range at constant vibration acceleration.

The first three resonant modes of the harvester device are around 65 Hz, 76 Hz and 220 Hz, respectively. It is seen from the experimental result in Fig. 5 that unlike a linear oscillation system, the output voltage shows a broadband response instead of three voltage peaks. It is because the beam stretching induced nonlinearity broadens the resonance of 65 Hz towards a higher bandwidth range. The broadened resonance overlaps successively with the second and third resonance modes, i.e. 76 Hz

and 220 Hz. Such interaction further enables the resonance to extend towards an ultra high resonance. At an acceleration of 0.5g, as the excitation frequency sweeps up, the resonance is pushed towards a high-energy stable region until  $A_1$  at 340 Hz. After that, the instability overcomes the nonlinear stiffness effect of the system and thus the oscillation jumps down from the high-energy state to a low-energy state. Comparing to the resonance of the frequency down-sweep response (93 Hz at  $A_2$ ), the operating bandwidth is widely broadened of 365%. Similarly, as the acceleration increases to 1.0g, the resonance of 400 Hz at  $B_1$  for frequency up-sweep is much higher than that of 230 Hz at  $B_2$  for frequency down-sweep. The peak voltage at points  $A_1$  and  $B_1$  are obtained as 0.19 mV and 0.24 mV, respectively. The corresponding peak powers are obtained as 0.18 nW at point  $A_1$  and 0.3 nW at point  $B_1$ , with respect to the match load resistance of 195  $\Omega$ .



#### 4. Conclusion

In this paper, an ultra-broadband electromagnetic MEMS energy harvester is fabricated and characterized. Comparing to frequency down-sweeps, the bandwidth is 365% and 174% wider than frequency up-sweeps. It is due to the nonlinear beam stretching at the first three resonant modes, the operating bandwidth is extended from the original resonant frequency of 65 Hz to be as wide as 340 Hz at 0.5g and 400 Hz at 1.0g.

#### References

- [1] J. A. Paradiso, T. Starner 2005 *IEEE Pervas. Comput.* **4** 18-27
- [2] S. P. Beeby, M. J. Tudor, N. M. White 2006 *Meas. Sci. Technol.* **17** R175-95
- [3] D. Zhu, M. J. Tudor, S. P. Beeby 2010 *Meas. Sci. Technol.* **21** 022001
- [4] S. D. Nguyen, E. Halvorsen 2011 *J. Microelectromech. Syst.* **20** 1225-7
- [5] X. Xing, J. Lou, G. M. Yang, O. Obi, C. Driscoll, N. X. Sun 2009 *Appl. Phys. Lett.* **95** 134103
- [6] S. C. Stanton, C. C. McGehee, B. P. Mann 2009 *Appl. Phys. Lett.* **17** 174103
- [7] M. S. M. Soliman, E. M. Abdel-Rahman, E. F. El-Saadany, R. R. Mansour 2008 *J. Micromech. Microeng.* **18** 115021
- [8] L. G. W. Tvedt, D. S. Nguyen, E. Halvorsen 2010 *J. Microelectromech. Syst.* **19** 305-16
- [9] A. Hajati, S.-G. Kim 2011 *Appl. Phys. Lett.* **17** 174103
- [10] H. Liu, C. J. Tay, C. Quan, T. Kobayashi, C. Lee 2011 *J. Microelectromech. Syst.* **20** 1131-42
- [11] H. Liu, C. Lee, T. Kobayashi, C. J. Tay, C. Quan 2012 *Microsyst. Technol.* **18** 497-506
- [12] D. Miki, M. Honzumi, Y. Suzuki, N. Kasagi 2010 *IEEE MEMS 2010* 176-9
- [13] D. S. Nguyen, E. Halvorsen, G. U. Jensen, A. Vogl 2010 *J. Micromech. Microeng.* **20** 125009